Synthesis and Characterization of Bulk and Thin Film Clathrates for Solid State Power Conversion Applications

Sarath Witanachchi, Robert Hyde, Matt Beekman, Devajyoti Mukherjee, Pritish Mukherjee, and George S. Nolas
Department of Physics, University of South Florida, Tampa, Florida 33620, USA
E-mail: switanac@cas.usf.edu

Abstract

Thin films of the type I clathrate $Ba_8Ga_{16}Ge_{30}$ have been synthesized by the pulsed laser ablation technique. The relatively low ablation threshold of this material at the UV wavelength leads to the ejection of particulates during laser-target interaction. The optimum laser fluence for the formation of stoichiometric films with the lowest particle density was 2.5 J/cm^2. Excitation of the UV laser generated plasma by a second pulsed CO_2 laser further reduced particulate ejection and produced broader expansion profiles leading to large area uniform films. Films deposited by this method on quartz substrates were polycrystalline and showed semiconducting behavior. High purity type II Na_xSi_{136} clathrates in bulk form have been synthesized by solid state reactions. The electrical properties of Na_xSi_{136} ($0 < x < 24$) clathrates show a clear dependence on Na content, with resistivities that span several orders of magnitude.

Introduction

Inorganic clathrate compounds [1] comprise a class of materials in which covalently bonded frameworks encapsulate loosely bonded atoms or molecules, commonly referred to as 'guests.' In addition to the unique and interesting crystal structures these materials possess, the relationship between these guests and the 'host' framework plays a crucial role in determining the various physical properties of the clathrates. Thus clathrates display varied behavior as metals, [2, 3] semiconductors, [4] and even sp^3 bonded superconductors [5].

Most of the work on inorganic clathrates to date has been centered on the type I and type II structures. These structure types are characterized by the atomic polyhedra that share faces to form their covalently bonded frameworks. In type I clathrates, two pentagonal dodecahedra and six tetrakai-decahedra per conventional unit cell form the framework (Fig. 1a). This allows for the accommodation of eight guests per formula unit, which can be written as A_8E_{46}. Here A and E represent the guest and framework atoms, respectively. In type II clathrates, the framework is formed by sixteen pentagonal dodecahedra and eight hexakaidecahedra per conventional unit cell (Fig. 1b). In contrast to type I clathrates, type II clathrates allow for partial occupation of the polyhedra, up to a total of twenty-four guests per formula unit, which can be written as A_xE_{136} ($0 < x < 24$).

One of the more interesting properties of clathrates is their low thermal conductivity, and in some cases they possess the thermal properties characteristic of amorphous materials. For example, type I clathrates such as $Sr_8Ga_{16}Ge_{30}$ and $Eu_8Ga_{16}Ge_{30}$ possess very low thermal conductivities, with temperature dependences that actually mimic those of glasses such as amorphous SiO_2 [6]. This phenomenon has been very well explained by the interaction of the host framework heat-carrying phonons with the localized vibrational modes of the guests which may scatter the former [6, 7]. In addition to their low thermal conductivities, some semiconducting inorganic clathrates have shown promising thermoelectric properties, [4] sparking much interest in this field [8]. The low thermal conductivity combined with the relatively high power factors reported at high temperature for clathrates such as $Sr_8Ga_{16}Ge_{30}$ [9] and $Ba_8Ga_{16}Ge_{30}$ [10] are reasons why these materials continue to be actively investigated in the field of thermoelectrics.

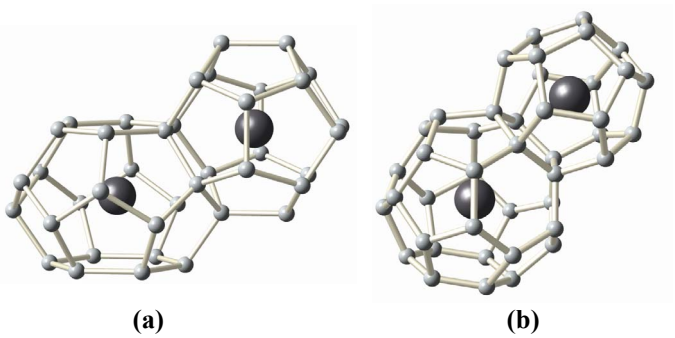

(a) **(b)**

Figure 1: The framework polyhedra that form (a) the type I clathrate structure and (b) the type II clathrate structure. The framework atoms are shown in light grey, while the guest atoms are shown in dark grey.

Clathrates have also attracted attention as potential photovoltaic and optoelectronic materials. Recently, it was shown [11] that a completely empty type II clathrate Si_{136} can be prepared, and this material was shown to possess a wide 2 eV band-gap. Efficient absorption of radiation in the optical region of the spectrum by this material would offer a new direction in the search for novel optoelectronic and photo-voltaic materials that would be compatible with currently established silicon technology.

As a result of the interesting properties and technological promise of type I and type II clathrates, the bulk properties of these materials have been studied extensively using a wide range of experimental and theoretical techniques. However, the production and characterization of stoichiometric clathrates in film form have not been studied extensively. In this paper we report the first results on the growth and structural characterization of germanium-based clathrate films of $Ba_8Ga_{16}Ge_{30}$ using pulsed laser ablation. One of the main advantages of laser ablation for film growth is the ability of this process to closely reproduce the target stoichiometry in the deposited film [12-14]. Therefore, laser ablation is uniquely suited for the growth of multi-component films from a single composite target such as $Ba_8Ga_{16}Ge_{30}$. In a typical

Authorized licensed use limited to: University of South Florida. Downloaded on December 9, 2009 at 12:51 from IEEE Xplore. Restrictions apply.

laser ablation process the laser-target interaction generates a plasma plume of the ablated species. The explosive nature of the ablation process gives rise to ejection of micron and submicron particulates of the target material. Particulate ejection is more pronounced for targets of metallic materials. We have used a dual-laser ablation process, where a pulsed CO_2 laser was used to further heat the plasma generated by the UV laser to re-evaporate the ejected particles, to produce films with a low density of defects.

Experimental Details

Type I clathrates used for laser ablation targets were prepared by mixing stoichiometric quantities of the high purity elements Ba (99%, Aldrich), Ga (99.9999%, Chameleon), and Ge (99.99%, Alfa Aesar). The mixtures were placed in pyrolytic boron nitride crucibles, and sealed in fused quartz ampoules under high purity nitrogen gas at a pressure of 2/3 atm. The mixtures were heated at 1°C/min to form $Ba_8Ga_{16}Ge_{30}$, held at 1000°C for 24 hours, and then cooled at a rate of 2°C/min. Targets for ablation were produce by hot and cold pressing procedures to a compacted density of higher than 95% of the theoretical X-ray density, as analyzed by powder X-ray diffraction (XRD). The preparation of bulk type II Na_xSi_{136} clathrates is discussed previously [15].

The laser ablation system used for film growth is shown in Figure 2. In the single laser ablation process excimer laser pulses (wavelength of 248 nm and duration 25 ns) are focused onto the target placed in a 10^{-7} torr vacuum. Laser-target interaction generates a plasma plume of the target species that expands into the vacuum. The plume is allowed to deposit on a heated substrate placed about 6 cm from the target. For dual-laser ablation, a CO_2 laser with a pulse duration of 250 ns and wavelength of 10.06 μm was focused in a glancing incidence configuration onto the plasma just above the target surface. The percentage of the CO_2 laser absorbed by the plasma was measured by monitoring the transmitted pulse on a pyro-electric detector. The delay between the two lasers

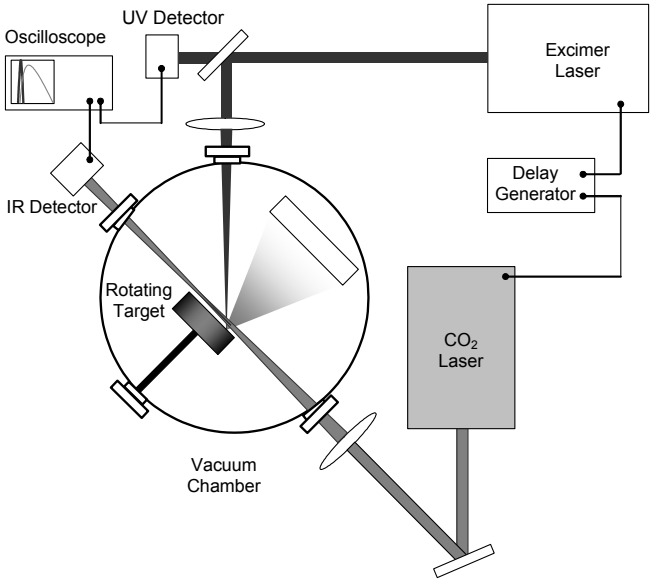

Figure 2: Dual-laser ablation system.

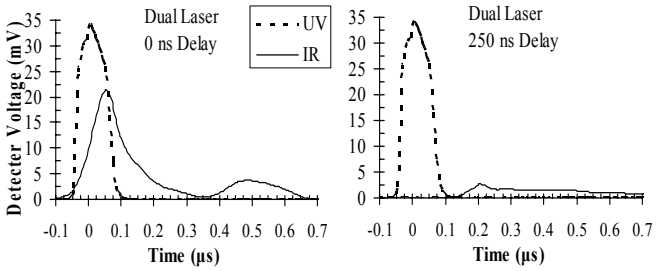

Figure 3: Oscilloscope traces of the excimer pulse (UV) and the CO_2 laser pulse (IR) after interaction with the plasma. At 250 ns delay, most of the CO_2 laser energy was absorbed.

was adjusted to obtain the maximum coupling of the CO_2 laser energy to the plasma. Films of $Ba_8Ga_{16}Ge_{30}$ were deposited on quartz substrates from room temperature to 600°C. The morphologies of the films were investigated by scanning electron microscopy (SEM) while the stoichiometry was studied by energy dispersive spectroscopy (EDS) analysis. Structural characterization of the films was done by XRD analysis.

Results and Discussion

At the excimer laser wavelength, ablation was observed for laser fluences as low as 0.5 J/cm^2. At low laser fluences the ion density and the energy of the evaporated species as well as the rate of film growth is significantly low. With increasing laser fluence the ion density of the plasma increases leading to enhanced absorption of the laser radiation into the plasma. This increases the plasma temperature that causes the particulates in the plasma to re-evaporate. However, for very high fluences density of particles ejected increases as well. The surface morphology of $Ba_8Ga_{16}Ge_{30}$ films deposited with laser fluences from 0.75 J/cm^2 to 3.0 J/cm^2 have been studied by SEM. Particulate density was relatively high for both low and high fluences while the lowest particulate density was observed for the intermediate fluence of 2 J/cm^2. If the plasma produced at this fluence is further heated by pumping it with a CO_2 laser pulse, further reduction in particulate ejection can be expected. Since the plasma absorption coefficient α is proportional to n_i^2/ν^3, where n_i is the plasma ion density and ν is the laser frequency, the long wavelength CO_2 laser radiation couples into the plasma more efficiently [12]. If the CO_2 pulse interacts with the plasma when the ion density is maximum, most of the CO_2 energy is absorbed into the plasma producing the highest plasma temperature. Figure 3 shows the oscilloscope traces of the transmitted laser pulse as the delay between the lasers was varied. The maximum coupling (absorption) was observed for a 250 ns delay. As seen in Figure 4, the comparison of single and dual-laser deposited films indicate that the majority of the small particles have been re-evaporated by the high temperature plasma produced by the dual laser process.

EDS analysis of films deposited from a $Ba_8Ga_{16}Ge_{30}$ target at room temperature contained the correct stoichiometry but lacked any crystallinity. As the substrate temperature is increased above 200°C, formation of the crystal structure was observed. The XRD spectrum of a film deposited at 400°C is shown in Figure 5. All the observed peaks correspond to the type I clathrate structure.

Authorized licensed use limited to: University of South Florida. Downloaded on December 9, 2009 at 12:51 from IEEE Xplore. Restrictions apply.

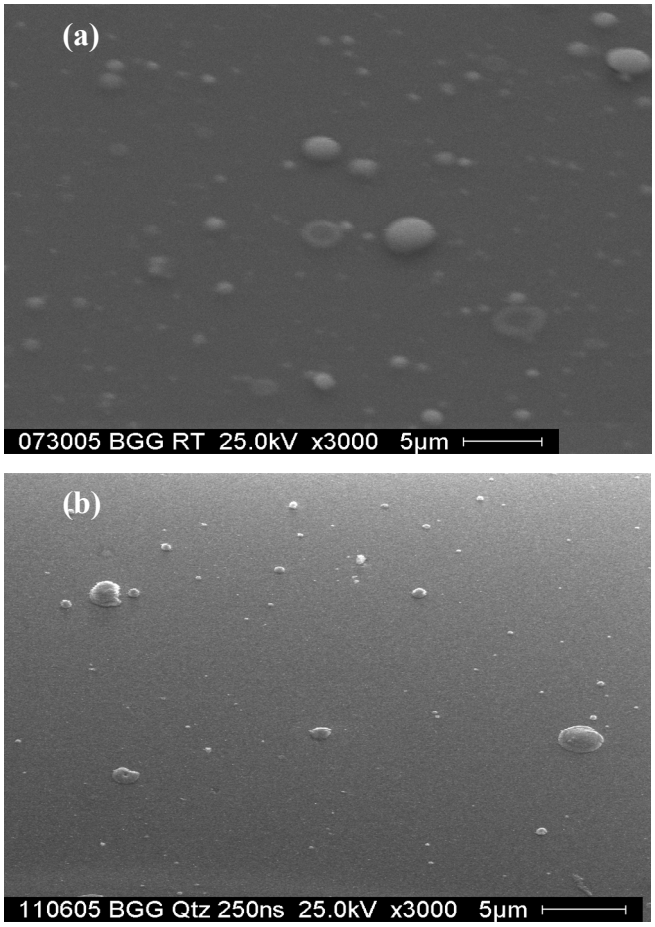

Figure 4: SEM mages of $Ba_8Ga_{16}Ge_{30}$ films deposited at laser fluences of 2.5 J/cm^2 by (a) single laser ablation and (b) dual-laser ablation.

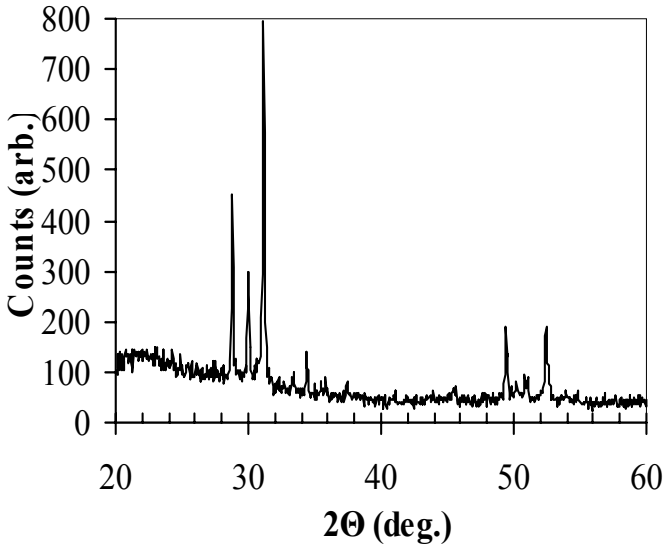

Figure 5: XRD spectra of a $Ba_8Ga_{16}Ge_{30}$ film deposited on quartz substrate at 400°C.

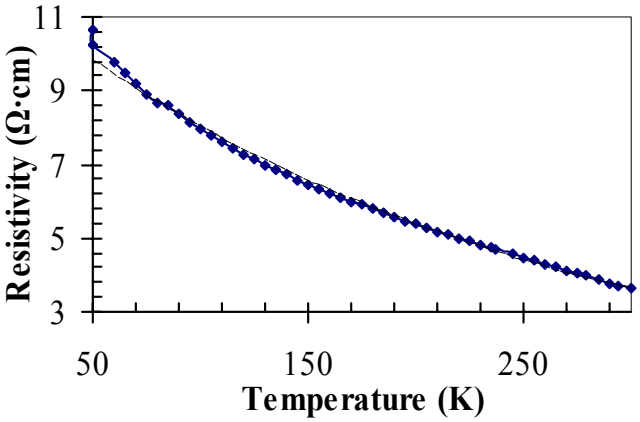

Figure 6: Temperature dependent resistivity for a $Ba_8Ga_{16}Ge_{30}$ film deposited at 400°C on quartz.

Temperature dependent electrical resistivity of the films was measured by a four-point probe technique in a custom built closed cycle refrigeration measurement system. Resistivity measurements from 300 to 50 K for a representative specimen are shown in Figure 6. The resistivity shows an activated behavior, indicative of a semiconductor. To our knowledge this is the first electrical measurement on a clathrate film to date.

In an effort to explore other clathrate structure types, we have recently begun a systematic investigation into the preparation and physical properties of bulk type II clathrates. [2, 15, 16, 17] Of particular interest in these materials is the ability to partially occupy the framework polyhedra, offering a route to control of the electrical and thermal transport properties in these materials. In particular, the thermal and electrical transport in type II Na_xSi_{136} clathrates has been found to be significantly affected by the guest content [15]. Figure 7 shows the electrical resistivities for three type II silicon clathrates. The clathrate $Cs_8Na_{16}Si_{136}$, which has all of the large polyhedra occupied by Cs and the small polyhedra occupied by Na, shows a resistivity with typical metallic temperature dependence [2]. In contrast, lower alkali content silicon clathrates such as Na_1Si_{136} and Na_8Si_{136} clearly exhibit large, activated resistivities [15]. A general trend is also apparent, where increasing the guest content reduces the magnitude of the resistivity, with a span of roughly 10^7 mOhm-cm at room temperature. This significant variation of the electronic properties with the guest content and type may allow for the "tuning" of their electrical properties for thermoelectric and photovoltaic applications. We are currently continuing this work with future efforts to include the synthesis and characterization of type II clathrate films.

Authorized licensed use limited to: University of South Florida. Downloaded on December 9, 2009 at 12:51 from IEEE Xplore. Restrictions apply.

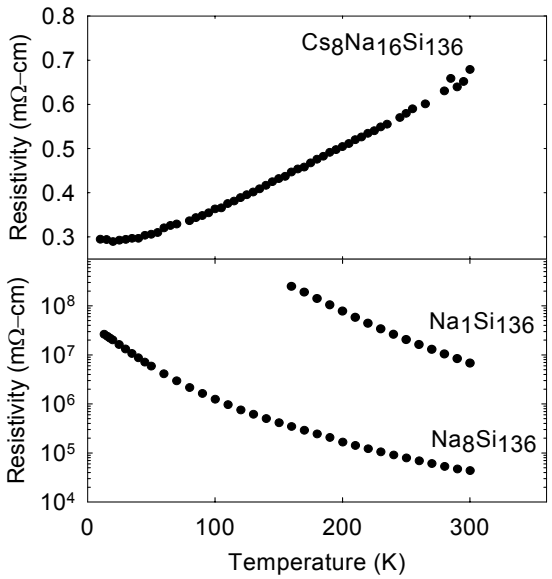

Figure 7: Electrical resistivity of $Cs_8Na_{16}Si_{136}$ [2] (top) as compared to Na_1Si_{136} and Na_8Si_{136} [14] (bottom).

Summary

We have successfully synthesized and characterized type I $Ba_8Ga_{16}Ge_{30}$ clathrates in film form using pulsed laser ablation techniques. The density of particulates ejected during growth has been reduced by coupling the energy of a CO_2 laser into the ablation plasma at the optimum inter-pulse delay. To the best of our knowledge, we have presented for the first time electrical measurements on a $Ba_8Ga_{16}Ge_{30}$ film, indicating the film is semiconducting. These results offer a new direction in which to study the properties of clathrates. Type II Na_xSi_{136} clathrates show electrical properties that depend strongly on the guest content, which may be varied in these materials, representing a potential optimization route for thermoelectric applications. The wide optical band gap of Na_xSi_{136} clathrates raises interest for optoelectronics and photovoltaic applications as well, and forms the impetus for our investigation into the production of thin films of these materials.

Acknowledgments

SW, RH, MB, PM and GSN acknowledge support by the US Department of Energy Office of Basic Energy Sciences, under Grant No. DE-FG02-04ER46145, on bulk and thin film clathrate research. SW and PM also acknowledge support from the National Science Foundation, under Grant No. DMI-0217939. MB gratefully acknowledges support from the University of South Florida Presidential Doctoral Fellowship.

References

1. Nolas, G.S., Slack, G.A., and Schujman, S.B., in Semiconductors and Semimetals, Ed. by T.M. Tritt, Academic (New York, 2001), pp. 255, and references therein.
2. Nolas, G.S., Vanderveer, D.G., Wilkinson, A.P., and Cohn, J.L., "Temperature dependent structural and transport properties of the type II clathrates $A_8Na_{16}E_{136}$ (A = Cs or Rb and E = Ge or Si)," *J. Appl. Phys.* **91**, (2002) 8970.
3. Nolas, G.S., Ward, J.-M., Gryko, J., Qui, L., and White, M.A., "Transport properties of Na_8Si_{46}," *Phys. Rev. B* **64**, (2001) 153201.
4. Nolas, G.S., Cohn, J.L, Slack, G.A., and Schujman, S.B., "Semiconducting Clathrates: Promising candidates for thermoelectric applications," *Appl. Phys. Lett.* **73**, (1998)178.
5. Kawaji, H., Horie, H., Yamanaka, S., and Ishikawa, M., "Superconductivity in the Silicon Clathrate Compound $(Na,Ba)_xSi_{46}$," *Phys. Rev. Lett.* **74**, (1995) 1427.
6. Cohn, J.L, Nolas, G.S., Fessatidis, V., Metcalf, T.H., and Slack, G.A., "Glasslike Heat Conduction in High-Mobility Crystalline Semiconductors," *Phys. Rev. Lett.* **82**, (1999) 779.
7. Nolas, G.S., Weakley, T.J.R., Cohn, J.L., and Sharma, R., "Structural properties and thermal conductivity of crystalline clathrates," *Phys. Rev. B* **61**, (2000) 3845.
8. See, for example, Thermoelectrics Handbook: Macro to Nano, Ed. by D.M. Rowe, CRC Press (Boca Raton, 2006).
9. Nolas, G.S., "Structure, Thermal Conductivity, and Thermoelectric Properties of Clathrate Compounds," in Thermoelectrics Handbook: Macro to Nano, Ed. by D.M. Rowe, CRC Press (Boca Raton, 2006), pp. 33-1.
10. Saramat, A. et al., "Large thermoelectric figure of merit at high temperature in Czochralski-grown clathrate $Ba_8Ga_{16}Ge_{30}$," *J. Appl. Phys.* **99**, (2006) 023708.
11. Gryko, J., McMillan, P.F., Marzke, R.F., Ramachandran, G.K., Patton, D., Deb, S.D., and Sankey, O.F., "Low-density framework form of crystalline silicon with a wide optical band gap," *Phys. Rev. B* **62**, (2000) R7707.
12. Witanachchi, S., Ahmed, K., Sakthivel, P., and Mukherjee, P., "Dual-laser ablation for particulate-free film growth *Appl. Phys. Lett.* 66, (1995) 1469.
13. Mukherjee, P., Cuff, J.B., and Witanachchi, S., "Plume expansion and stoichiometry in the growth of multi-component thin films using dual-laser ablation," *Appl. Surface Sci.* **127-129**, (1998) 620.
14. Mukherjee, P., Chen, S., Cuff, J.B., Sakthivel, P., Witanachchi, S., "Evidence for the physical basis and universality of the elimination of particulates using dual-laser ablation. I. Dynamic time-resolved target melt studies, and film growth of Y2O3 and ZnO," *J. Appl. Phys.* **91**, (2002) 1828.
15. Beekman, M., and Nolas, G.S., "Synthesis and thermal conductivity of type II silicon clathrates," *Physica B* (in press).
16. Nolas, G.S., Kendziora, C.A., Gryko, J., Dong, J., Myles, C.M., Poddar, A., and Sankey, O.F., "Raman scattering study of stoichiometric Si and Ge type II clathrates," *J. Appl. Phys.* **92**, 7225 (2002).
17. Nolas, G.S., Beekman, M., Gryko, J., Lamberton, Jr., G.A., Tritt, T.M., and McMillan, P.F., "Thermal conductivity of elemental crystalline silicon clathrate Si_{136}," *Appl. Phys. Lett.* **82**, (2003) 910.

Authorized licensed use limited to: University of South Florida. Downloaded on December 9, 2009 at 12:51 from IEEE Xplore. Restrictions apply.